JOURNAL OF APPLIED ELECTROCHEMISTRY 14 (1984) 555–564

Enhanced mass transfer at the rotating cylinder electrode. I. Characterization of a smooth cylinder and roughness development in solutions of constant concentration

D. R. GABE, F. C. WALSH*

Department of Materials Engineering and Design, University of Technology, Loughborough, Leicestershire, LE11 3TU, UK

Received 21 February 1983; revised 24 October 1983

A versatile rotating cylinder electrode (RCE) assembly has been constructed in order to study the development of surface roughness during the prolonged cathodic deposition of metal at high overpotential. The initial smooth cylindrical surface and its behaviour have been characterized and the onset of rough deposits is described by an empirical power law (based on the mass transfer correlation) I_L = (constant) U^x where $x \simeq 0.74$ for a smooth surface and $x \simeq 0.90$ for a roughened surface. The uses and limitations of this power law are discussed.

Nomenclature

		Typical units
a, b, c	constants in Equation 1	–
A	active area of rotating cylinder	cm^2
C	concentration	$mol\,cm^{-3}$
d	diameter of rotating cylinder	cm
D	diffusion coefficient	$cm^2\,s^{-1}$
F	Faraday constant	96 487 C mol^{-1}
I_0	useful current (Equation 2)	A
I_L	limiting current	A
j'_D	mass transport factor ($= St\,Sc^c$)	–
K	constant in Equation 2	–
p	velocity exponent for powder formation	–
R_a	average roughness	μm
U	peripheral velocity of cylinder	$cm\,s^{-1}$
t	time	s
z	number of electrons	–
Re	Reynolds number $= \frac{Ud}{\nu}$	–
Sc	Schmidt Number $= \frac{\nu}{D}$	–
St	Stanton Number $= \frac{I_L}{AzFCU}$	–
ν	kinematic viscosity	$cm^2\,s^{-1}$
x	velocity exponent	–

1. Introduction

The advantages of the rotating cylinder electrode (RCE) have been well-rehearsed recently [1–3] but may be summarized in terms of high mass transfer in turbulent flow at low rotation rates, an equipotential surface for potentiostatic control, good solution mixing in a relatively low volume cell and versatility of design for continuous cascade reactor usage. The development of the RCE as a metal recovery reactor is more widespread than might be imagined [2]. This can be partly attributed to Holland [4, 5] who envisaged a continuous process for stripping off metal from various liquors and depositing it as a powdered cathode product which may be continuously

* Now at the Wolfson Centre for Electrochemical Science, Department of Chemistry, University of Southampton, Southampton, SO9 5NH, UK.

0021–891X/84 $03.00 + .12

or intermittently removed from the electrode surface.

The mass transfer behaviour of a smooth RCE was first studied in depth by Eisenberg *et al.* [6, 7] who proposed a dimensionless correlation of the type:

$$St = aRe^{b}Sc^{c} \quad (1)$$

(where $a = 0.079$, $b = -0.30$, $c = -0.644$). Subsequent studies have shown this to be essentially correct [2, 8, 9] with only small variations in the values of a, b and c. Previous work on rough surfaces has been reported by Kappesser *et al.* [10, 11], Theodorsen and Regier [2], Sedahmed *et al.* [13, 14] and others, and has been considered in detail elsewhere [2]. In particular, Holland [4, 5, 15] has reported that when the cathode product is a metal powder, enhanced mass transfer can be attained which can be empirically described by a power law of the form:

$$I_0 = KCU^{x} \quad (2)$$

Under mass transport control, I_0, the useful current [4, 5] may be identified with I_L, the limiting current under the prevailing conditions. For a smooth cylinder the power index $x \simeq 0.7$ but as powder forms $x \rightarrow p$ which typically has a value of 0.92. Such enhanced mass transfer is highly advantageous to a reactor process such as the ECO-CELL*; it is not an example of 'super-turbulence' but an instance of increased surface micro-turbulence (due to greater hydrodynamic shear) combined with a marked increase in *active* surface area. Equation 2 is therefore empirical although highly convenient for design purposes within a well-defined range of conditions. Strictly, this equation relates specifically to copper deposition from acidic solutions [15]. Equation 2 has also been expressed in the form of an empirical, dimensionless correlation:

$$St = 0.079Re^{-0.08}Sc^{-0.644} \quad (3)$$

This investigation has attempted to study the enhanced mass transport attainable during the growth of rough metal deposits onto a well characterized and initially smooth RCE.

* ECO-CELL is a registered trademark of Ecological Engineering Ltd, now a part of Steetley Engineering Ltd, Brierley Hill, West Midlands, UK. The device is a commercially available RCE, normally acting in a continuous metal powder producing mode, for the treatment of dilute metal bearing liquors.

2. Experimental details

2.1. *The RCE reactor cell*

In designing a laboratory-scale reactor, two conflicting requirements had to be reconciled: the RCE cell had to be capable of performing in reproducible, precise conditions to provide definitive mass transport data while also performing as a scaled-down model of the commercial ECO-CELL plant. For design and construction purposes, the reactor had to be:

(a) constructed from corrosion resistant materials and be capable of being readily dismantled, assembled and adapted to a variety of solutions;

(b) capable of being divided by an ion exchange membrane exploiting insoluble anodes in an idealized anolyte while copper soluble anodes could be used in an undivided mode;

(c) sealed and vented to minimize vortex formation and uncontrolled gas venting, and also be operated under thermostatic conditions;

(d) such that it could operate in simple batch, single pass and batch recycle modes with good flow-through behaviour;

(e) of a geometry which could promote uniform cathode potential and current density when the cylinder was potentiostatically controlled.

A schematic diagram is shown in Fig. 1 and illustrates the construction based on Tufnol platforms supported by four nickel-plated steel rods bolted at each level. A Servomex Controls motor ($\frac{1}{8}$ hp type MC43), equipped with tachometer feedback control, enabled rotational speeds of 180–1500 r.p.m. ± 1% to be employed, a wider range being available at higher levels of error. The motor was coupled to the stainless steel drive shaft by a flexible nylon sleeve on which a contact slip ring, silver plated for high duty service, was fixed with a locking taper. Power was provided through two silver-filled graphite brush assemblies, each of approximately 8 cm^2 in area, the interface being well run in and lubricated with colloidal graphite. A linear tachometer provided 1.0 V output at 1000 r.p.m. and was fully calibrated. A second brush assembly was provided nearer the RCE to provide a potential sensing contact for the potentiostat.

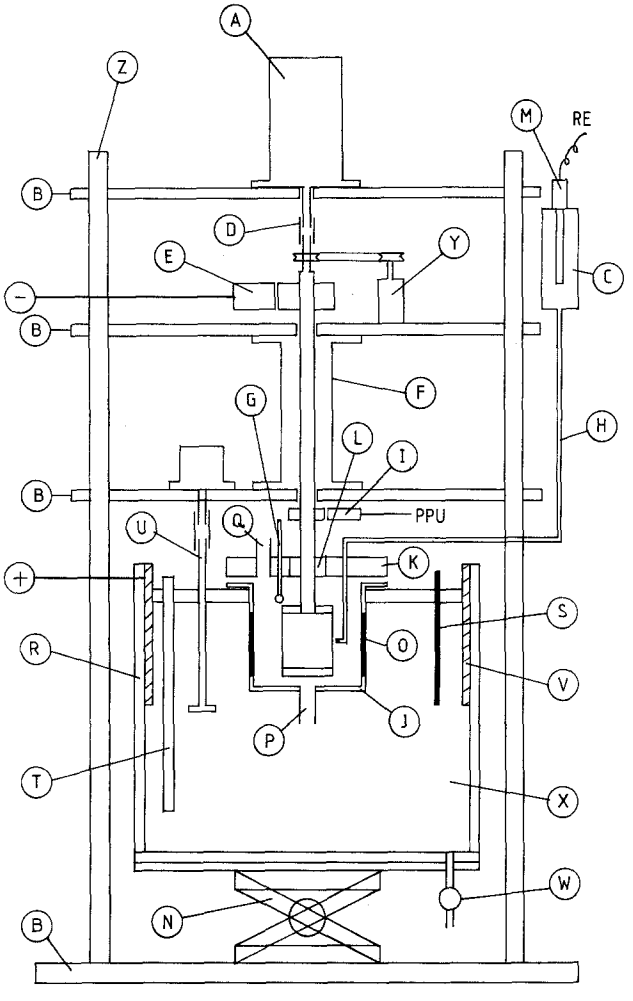

Fig. 1. Schematic of the completed laboratory rotating cylinder electrode reactor assembly. (A) Electric drive motor; (B) 'Tufnol' support platform (4); (C) Salt bridge reservoir; (D) Flexible nylon drive coupling; (E) Power brushes (2) and slip ring; (F) Bearings housing; (G) Catholyte thermometer; (H) Reference electrode salt bridge; (I) Potential pick-up brush; (J) 'Perspex' catholyte chamber; (K) 'Perspex' catholyte chamber top plate; (L) Catholyte/rotating shaft seal; (M) Reference electrode; (N) Anolyte chamber elevating jack; (O) Cation exchange membranes (4); (P) Catholyte inlet; (Q) Catholyte outlet; (R) 'Perspex' anolyte chamber; (S) Anolyte thermostat; (T) Anolyte heater (2); (U) Anolyte stirrer; (V) Plate lead anode (4); (W) Anolyte drain tap; (X) Sulphuric acid anolyte; (Y) Auxiliary tachometer; (Z) Steel support rods (4).

The top plate of the reactor cell was provided with several sealable apertures designed to accept reference electrodes, thermometers, etc., as well as the rotating shaft. The perspex top plate was sealed to the reactor body using nitrile 'O' ring seals, and was secured by eight quick release stainless steel thumb-screws. For flow-through operation, polypropylene tubes and fittings were used.

The reactor body was essentially a catholyte compartment set in a large anolyte tank serving a dual role as a thermostatically controlled reservoir. Each side of the approximately cubic catholyte tank was fitted with a sheet of cationic exchange membrane (Ionac MC3 470) sealed with gaskets and polypropylene fasteners, and providing four windows each of 8 cm x 8 cm area. The anolyte compartment was provided with two 500 watt silica-sheathed immersion heaters, rotational stirrers and anode connections. In normal usage four Pb–6% Sb alloy plate anodes, each of 100 cm^2 area, were used in an anolyte of 1.5 M sulphuric acid, the large gap giving rise, of course, to relatively large voltage drops but otherwise even current distribution. In soluble anode experiments a copper foil anode was mounted inside the catholyte chamber which then acted as an undivided reactor. Catholyte solutions could be prepared in and recirculated from a 20 dm^3 thermostatically heated reservoir; the flow rate was controlled by throttle valves together with a variable speed peristaltic pump.

The electrode itself comprised a stainless steel cylinder (6 cm diameter x 6 cm long) provided with insulating end caps (6 mm thick) of PTFE designed to promote uniform hydrodynamic con-

ditions at each end and to minimize any edge effects. This cylinder was attached to the shaft via a male thread on the upper end and could be removed for cleaning, remachining or replacement by duplicate cylinders knurled to provide standardized initial roughnesses. In an alternative design, seamless foil-tube could be slid over the smooth cylinder and held securely in place by a modified pair of end caps.

2.2. *Procedure*

Laboratory solutions were prepared volumetrically using AR grade chemicals in a background electrolyte of 1.5 M H_2SO_4, a typical concentration would be 0.014 M $CuSO_4$, equivalent to a copper level of 890 ppm. Copper analysis was performed by atomic absorption spectrophotometry, negligibly small samples of electrolyte being withdrawn from the cell at suitable intervals.

The apparatus was fully instrumented, as shown schematically in Fig. 2, and temperatures were maintained in the range 20–60° C to within ± 0.5° C. Potentiostatic control was provided by a Chemical Electronics power source of 20 V/50 A capacity, the current being recorded on a Bryans Model 28 000 potentiometric chart recorder. Both cell voltage and cathode potential were continuously monitored. The latter was made with reference to a saturated mercury/mercurous sulphate reference electrode (SSE) fitted to a ceramic frit probe and 1 M Na_2SO_4 reservoir to provide an adjustable hydrostatic head. Such a sulphate reference electrode was preferred to the normal calomel form in order to avoid possible chloride contamination. Potentiodynamic sweeps were generated by a Chemical Electronics unit; the usual sweep rate was 1 mV s^{-1} over an overpotential range of 0–700 mV which gave a cathode polarization curve in less than 12 min.

The stainless steel cylinder surface was prepared by successive treatments: polishing with wet 600 grade emergy paper, degreasing in 1,1,1-trichlorethane and preplating potentiostatically

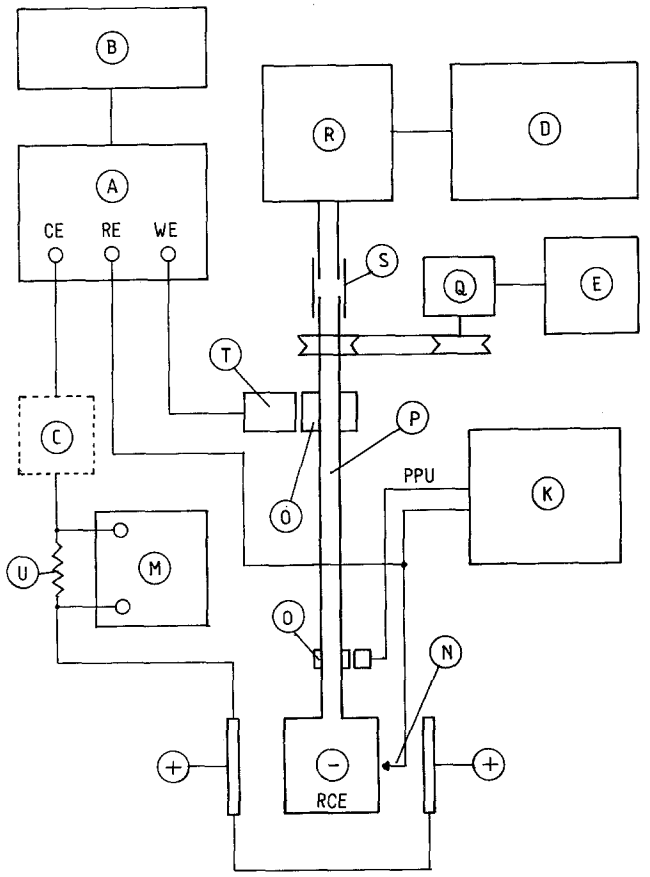

Fig. 2. Schematic of the electrical circuitry for the laboratory reactor. (A) Potentiostat; (B) Linear sweep unit; (C) Digital coulombmeter (optional); (D) Rotating cylinder speed control; (E) Auxiliary tachometer; (K) High impedance millivoltmeter; (M) Chart recorder; (N) Reference electrode assembly; (O) Slip rings (2); (P) Rotating shaft; (Q) Auxiliary tachometer sender; (R) Rotating shaft drive motor; (S) Flexible nylon drive; (T) Cathode power brush; (U) Precision shunt; (RCE) Rotating cylinder electrode; (WE) Working electrode; (CE) Counter electrode; (RE) Reference electrode; (PPU) Potential pick up.

with copper at a low overpotential for 60 s to yield an active, compact and adherent surface which was reproducible. Deposits were stripped chemically in 50% w/w nitric acid.

Mass transfer studies were accomplished by using a range of rotation rates to influence the limiting current densities determined potentiodynamically. Constant copper concentration trials were made using a combination of soluble copper anodes and a small flow through the cell in order to study developing roughness. Other variables which were investigated included the potential, electrode area and initial surface roughness.

The development of surface roughness was also studied directly by surface profilometry. The cylindrical electrode was detached from the shaft, rinsed and dried, mounted on a 'V' block table and subjected to stylus traversing profilometry (Rank–Taylor–Hobson Talysurf Model 10, 5 μm diamond stylus).

2.3. *Results*

Mass transfer data was obtained primarily by means of cathodic potentiodynamic measurements. Fig. 3 shows a typical family of steady state polarization curves indicating the effect of varying copper ion concentration (50–890 ppm) in 1.5 M H_2SO_4 at 22° C. It may be seen that with decreasing metal concentration the limiting current plateau becomes less well defined but there is relatively little effect in the low overpotential region where the reaction is not under mass transfer control. Rest potentials were measured by a high impedance DVM and became more negative with increasing copper dilution in a near Nernstian fashion. Using Fig. 3 and other similar data the mass transfer coefficient can be shown to remain constant as exemplified by the plots in Fig. 4 which shows that at 500 r.p.m. the mass transport coefficient is 3.3×10^{-3} cm s^{-1} and Relation 4 is a good approximation.

$$I_L = \text{constant} \cdot C \qquad (4)$$

A similar family of polarization curves showed the effect of rotational speed which may be alternatively represented by current–rotation speed curves at constant potential (Fig. 5). One can see that the effect of rotation speed becomes more marked as the overpotential is raised (i.e. mass

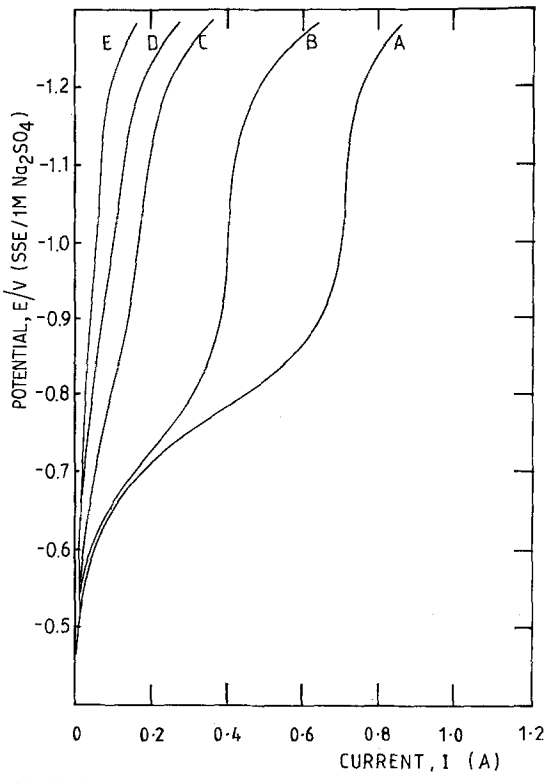

Fig. 3. Cathodic polarization curves for copper deposition onto smooth rotating cylinder electrodes, showing the effect of copper concentration: (A) 890, (B) 500, (C) 200, (D) 125, (E) 50 mg dm^{-3} Cu. Conditions: 1.5 M H_2SO_4; 22° C; 500 rpm; $d = 6.3$ cm; $l = 4.3$ cm; $A = 85.1$ cm^2; $U = 165$ cm s^{-1}; 2.5 mV s^{-1} linear sweep rate.

transfer becomes predominant) until at −1000 mV (vs SSE/1 M Na_2SO_4 electrode) a straight line is obtained in accordance with

$$I_L = \text{constant} \cdot U^{0.74} \qquad (5)$$

The effect of surface area was investigated by masking different proportions of the smooth cylinder to give effective lengths of 5.05, 4.3, 2.15 and 1.1 cm and, as expected, the area was proportional to the limiting current, the average current density being 8.1 mA cm^{-2}.

Potentiostatic control of the RCE may be employed for several purposes. In a separate study [16, 17] it has been shown that controlled separation of metals in solution can be achieved in certain cases by selecting appropriate cathodic deposition potentials. In this investigation the electrode was potentiostatically controlled at − 1000 mV (SSE/1 M Na_2SO_4) for a period of

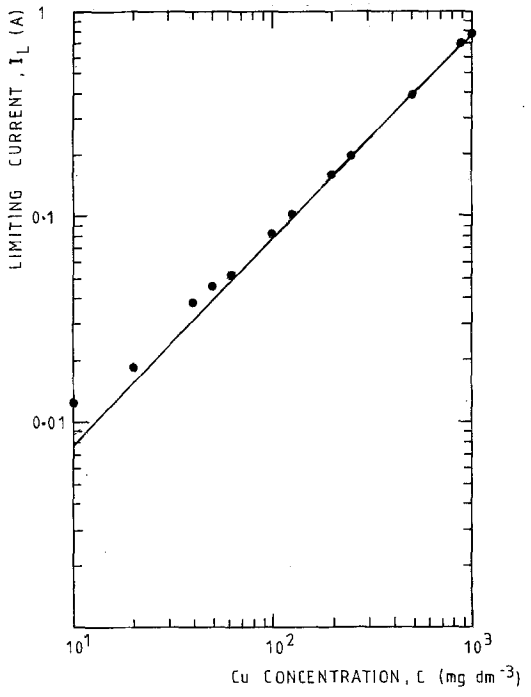

Fig. 4. Limiting current as a function of copper concentration; solid line corresponds to Equation 7 (conditions as in Fig. 3).

time using a fixed electrolyte concentration, typically 0.014 M $CuSO_4$ + 1.5 M H_2SO_4 at 22° C and various cylinder rotation rates (100–1000 r.p.m.). From the data obtained (Fig. 6) it can be seen that the I_L/t curves may be divided

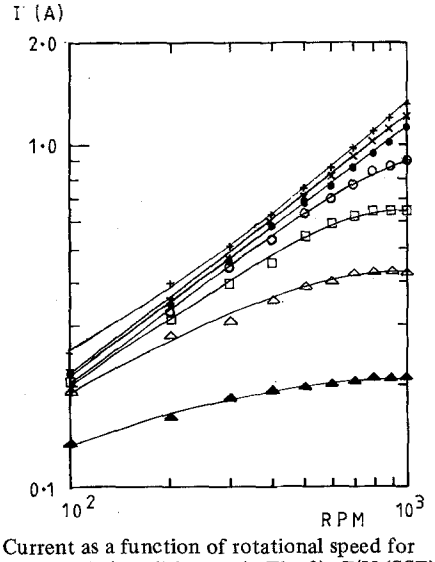

Fig. 5. Current as a function of rotational speed for various potentials (conditions as in Fig. 3). E/V (SSE) values: + 1.2; x 1.100; ● 1.000; ○ 0.900; □ 0.800; △ 0.700; ▲ 0.600.

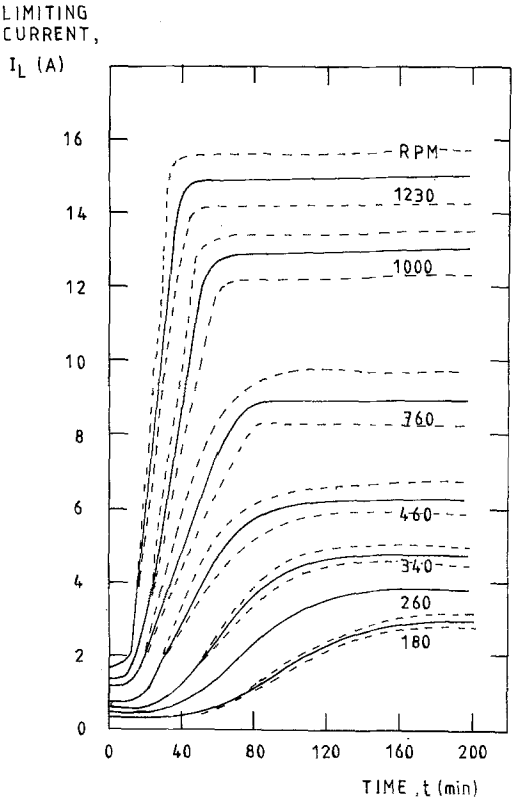

Fig. 6. Current–time history for growth of rough copper deposits showing the effect of rotational velocity with potentiostatic control at — 1.000 V SSE/1 M Na_2SO_4, corresponding to limiting current conditions: r.p.m. = 180–1230; U = 59.4–405.7 cm s^{-1}. The broken lines indicate the limits of reproducibility, typically for ten successive trials.

into three distinct regions for the purpose of discussion. Initially, the current corresponds closely to the limiting value obtained on a smooth RCE but after a critical time, which decreases with increasing rotation rate, the current progressively rises approaching an essentially steady value after a second critical time when a 'saturated' deposit roughness has been attained. Fig. 6 illustrates the limits of reproducibility for the data. Despite careful attention to the experimental conditions, noticeable variation in the final limiting currents was experienced. If a mass transfer plot is made, simplified in Fig. 7 to limiting current vs rotation rate, it may be seen that the initial 'smooth' cylinder data conforms to the relation:

$$I_L \propto U^{0.74} \qquad (6a)$$

(cf. Equation 5), whereas the 'saturated' roughness

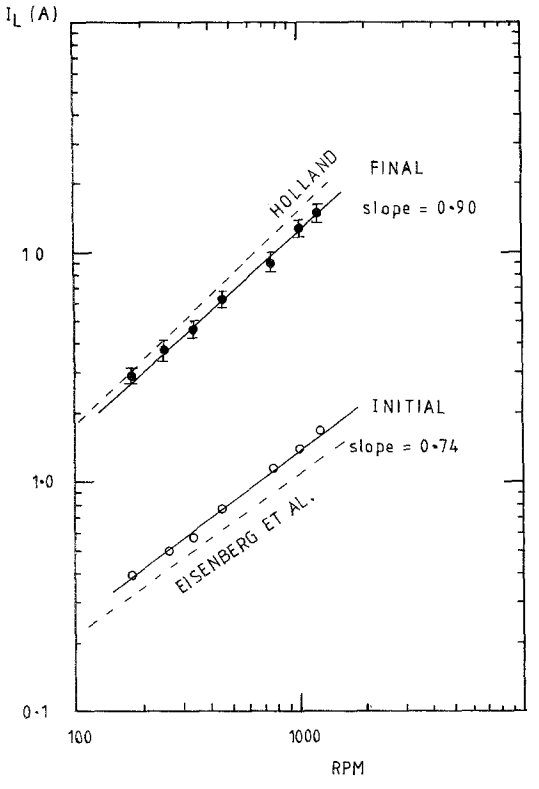

Fig. 7. Limiting current as a function of rotational velocity for smooth and roughened copper deposits corresponding to Fig. 6 initial and final limiting currents. The broken lines correspond to values predicted by known correlations, i.e. Holland (Equation 3) and Eisenberg *et al.* (Equation 7).

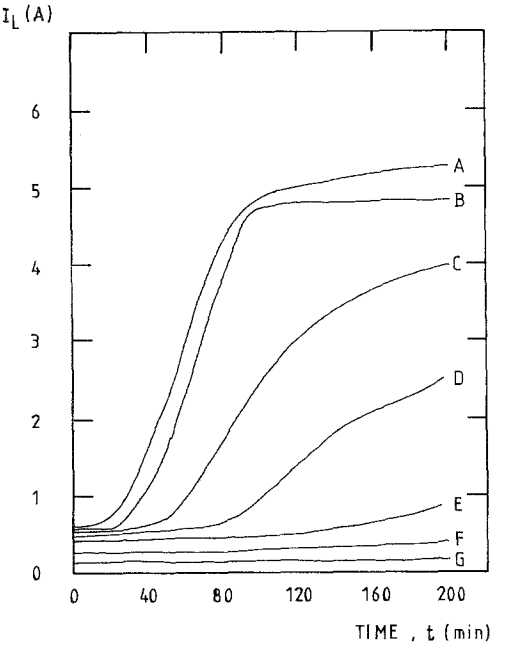

Fig. 8. Current–time curves during copper deposition showing the effect of cathode potential. Other conditions as for Fig. 3. E/V (SSE) values: (A) – 1.100; (B) – 1.000; (C) – 0.950; (D) – 0.900; (E) – 0.850; (F) – 0.750; (G) – 0.700.

state offers a correlation of the form

$$I_L \propto U^{0.90} \qquad (6b)$$

Potentiostatic control at lower potentials, i.e. below the value where a limiting current may be instantaneously produced, shows a less marked tendency to roughen but nevertheless will follow a similar pattern given sufficient time (Fig. 8). The development of roughness was measured by a Talysurf profilometer using a 5 μm diamond stylus with a 2 mN force for the same solution at two rotation speeds: 180 and 340 r.p.m. Although the reproducibility of the instrument for markedly three-dimensional nodular/powdery growths of this type is necessarily poor, the increase of roughness with time could clearly be seen (Fig. 9) and correlated with the increase in current observed in Fig. 7. Examination of the deposits in the scanning electron microscope revealed classical nodular growth patterns leading to powder formation in the manner investigated previously [8, 9].

3. Discussion

Although the polarization characteristics and the consequent pattern of mass transfer behaviour have been investigated [6–9], previous work has been limited to the study of smooth electrode surfaces either by avoiding growth of rough deposits [8, 9] or by using other electrode reactions including the ferro/ferricyanide redox couple [6, 7] and oxygen reduction [11]. In such circumstances it is always necessary to show that the dynamic system employed conforms in basic terms to that which is already known and understood. The steady-state polarization and potential sweep techniques employed here have shown this to be true in hydrodynamic conditions which are known to be turbulent and of a reproducible nature. One new feature of the cell used here, and an inherent feature of the ECO-CELL reactor, is the use of a diaphragm divider which most conveniently is incorporated in a non-concentric reactor geometry, in this instance, a square section. Early work has

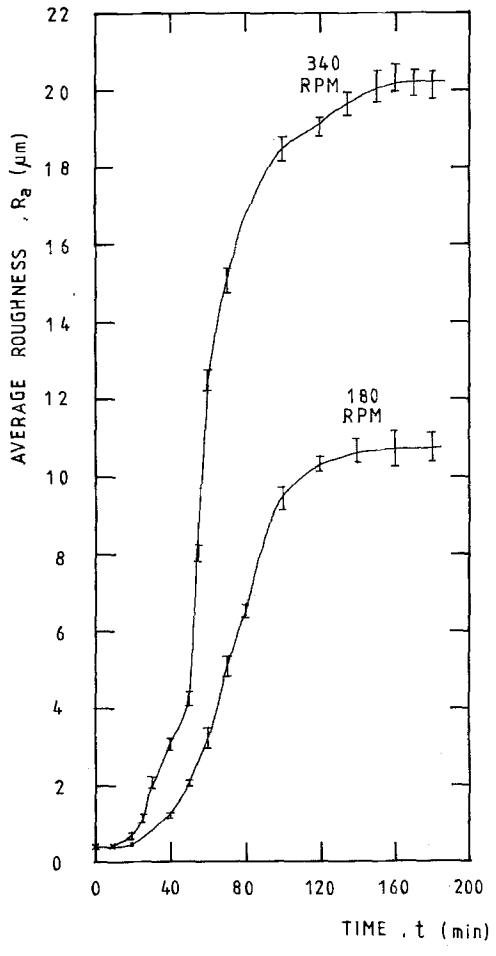

Fig. 9. Average roughness as a function of time for growth of rough deposits showing the effect of rotational speed with potentiostatic growth of copper at − 1.000 V (SSE/1 M Na_2SO_4). Conditions: r.p.m. = 180 or 340; U = 59.4 or 112.1 cm s^{-1}.

shown that the critical dimension is the diameter of the rotating cylinder [1, 2, 6, 7]; nevertheless, reassurance was vital before such a cell was employed to provide definitive mass transfer data. Therefore, a comparison of mass transfer data was sought using the limiting current data obtained under a range of conditions including variable rotation rates, temperatures, solution concentrations, etc. The results have been plotted (see Fig. 10) as $St \cdot Sc^{0.644}$ vs Re as predicted by Equation 1, and appear to lie between those of Eisenberg *et al.* [6, 7] and Robinson and Gabe [8, 9]. However, the difference is really quite small when it is realised that, in mathematical terms, the variation in the parameters is over a very narrow range in which some experimental features could appear exaggerated. Furthermore, previous workers have used different methods of statistical correlation which can, in themselves, cause slight discrepancies [1, 8, 9]. Thus, unless all previous data can be subjected to identical assessment, small changes in the power indices and constant must be accepted [18].

The importance of electrode geometry has received scant attention in the literature and in this respect the RCE is at a disadvantage compared with the rotating disc electrode for which the importance of electrode size and shape are well known. Furthermore, when used as a recirculating reactor, the effect of a volumetric flow must also be considered although it was found that low volumetric flow rates ($< 10\ dm^3\ min^{-1} \equiv$ nominal residence time of 10 s) had no significant effect on the limiting currents at constant concentration, a feature borne out in other work [2].

When the dimensionless correlation (Equation 1) is expressed in its fullest form:

$$K_L = \frac{I_L}{AzFCU} = 0.079 \left(\frac{Ud}{\nu}\right)^{-0.30} \left(\frac{\nu}{D}\right)^{-0.644} \quad (7)$$

the behaviour found, and illustrated in Figs. 4 and 6, can clearly be seen to be classical. At low concentrations an increasing contribution from a background current is inevitable, due both to Faradaic charging phenomena at the electrode and secondary cathodic reactions including reduction of dissolved oxygen or hydrogen evolution. The near-Nernstian behaviour of the smooth RCE rest potential may at first sight appear to be curious but in using the RCE as a reactor for stripping metal from waste solution it may be utilized as a *crude* indicator of copper concentration. The recorded values were found to be influenced by the nature of the surface, being more negative by up to 10 mV for freshly preplated rotating cylinders when compared to static foil electrodes.

The dependence of the mass transfer coefficient with rotation rate is often quoted as a criterion for mass transfer control of reactions. In this case it implies that $I_L \propto U^{1-b}$ where the value of b depends upon the electrode system used, the hydrodynamic regime employed and detailed variations in geometry, and the consequent flow pattern includes entry length effects if appropriate [19]. In this study roughness was allowed to

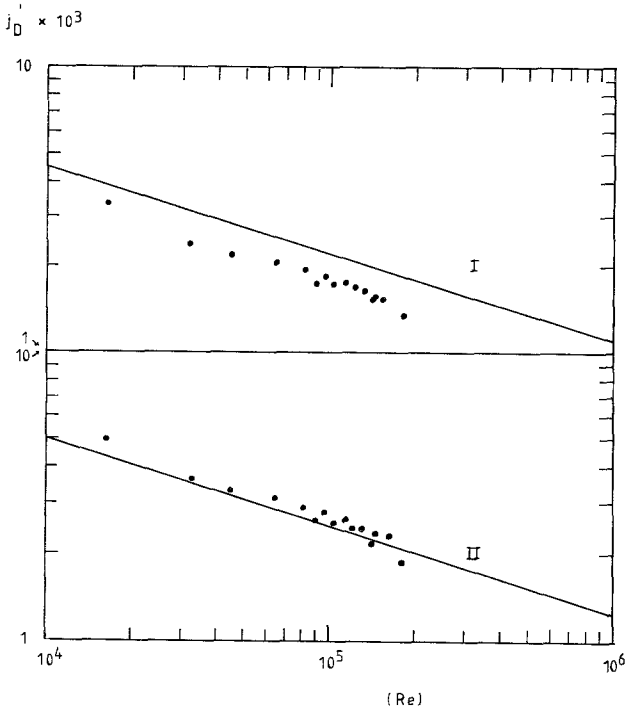

Fig. 10. Experimental mass transport data for copper deposition to a smooth rotating cylinder electrode. Comparison with known correlations. I. Eisenberg, Tobias and Wilke correlation: $j'_D = 0.079\,(\mathrm{Re})^{-0.30} = \mathrm{St}\,\mathrm{Sc}^{0.644}$. II. Robinson and Gabe correlation: $j'_D = 0.0791\,(Re)^{-0.31} = St \cdot Sc^{0.69}$

develop at constant copper ion concentration, ensured by the use of soluble anodes, in order to eliminate one possible variable. (It may be noted that in the ECO-CELL process under batch decay conditions, concentration normally falls as roughness develops leading to a powder deposit capable of being removed as such; this behaviour is studied in Part II.)

The form of the limiting current vs time curves (see Fig. 6) has already been described. Typically, at -1000 mV (SSE/1 M Na_2SO_4) the value of I_L increases almost tenfold, implying an increase in active surface area of a similar amount, but tends to a saturation value. The transition time to saturated roughness decreases markedly with increasing rotation rate when the initiation time has fallen to a very low value. Although roughness is known to develop as soon as nucleation occurs the use of a pretreated, i.e. prenucleated, electrode surface effectively eliminates this particular feature. While a degree of scatter in the results was observed, reproducibility was reasonable at short times implying a degree of randomness in the development of rough nodular growths. As it is not possible to make a true mass transfer correlation at this stage, onset of roughness has been identified by Holland [4, 5, 15] with a change of a power index in which he has assumed a relationship of the type $I_L \propto U^x$, with x increasing from 0.74 initially to 0.9 for a saturated roughness (Equations 5a, b).

The precision of these two values needs comment. Because the pretreated surface must necessarily have some slight roughness present the truly smooth surface should have a value of $x \simeq 0.7$ (Equation 6) and a value of 0.74 probably reflects this characteristic. The exponent for rough deposits is not well-established and in this study only seven points were obtained which were insufficient for statistical analysis. While there is evidence that $x \to 1.0$ as saturated roughness is achieved it suffices to say at this stage that if this simple power law is assumed the value of x undisputedly increases from 0.74 to 0.90. A more detailed consideration is made in Part II.

Acknowledgements

The authors are grateful to Professor I. A. Menzies for the provision of laboratory facilities. The studies were supported by an SRC CASE Award (to F.C.W.) in co-operation with Ecological Engineering Ltd, Macclesfield. Drs J. Overstall and R. J. Marshall of the Chemistry Department,

Southampton University, read the manuscript and made some helpful comments.

References

[1] D. R. Gabe, *J. Appl. Electrochem.* **4** (1974) 91.
[2] D. R. Gabe and F. C. Walsh, *ibid.* **13** (1983) 3.
[3] *Idem, Amer. Inst. Chem. Eng. Symp.* Cleveland, Ohio, 1982, to be published by the Electrochemical Society.
[4] F. S. Holland, British Patent 1 505 736 (1978).
[5] *Idem*, US Patent 4048199 (1977).
[6] M. Eisenberg, C. W. Tobias and C. R. Wilke, *Chem. Eng. Progr. Symp. Ser.* **51** (1955) 1.
[7] *Idem, J. Electrochem. Soc.* **101** (1954) 306.
[8] D. J. Robinson and D. R. Gabe, *Trans. Inst. Met. Fin.* **48** (1970) 35.
[9] *Idem, ibid.* **49** (1971) 17.
[10] R. Kappesser, I. Cornet and R. Greif, *J. Electrochem. Soc.* **118** (1971) 1957.
[11] I. Cornet and R. Kappesser, *Trans. Inst. Chem. Eng.* **47** (1969) T194.
[12] T. Theodorsen and A. Regier, NACA Report No. 793 (1944).
[13] G. H. Sedahmed, A. Abdel-Khalik, A. M. Abdallah and M. M. Farahat, *J. Appl. Electrochem.* **9** (1979) 563.
[14] *Idem, ibid.* **9** (1979) 567.
[15] F. S. Holland, *Chem. Ind.* (1978) 453.
[16] D. R. Gabe and F. C. Walsh, Proceedings of Interfinish '80, Kyoto, Japan (1980) p. 486.
[17] *Idem, Surf. Technol.* **12** (1981) 25.
[18] F. C. Walsh, PhD Thesis, Loughborough University of Technology, 1981.
[19] J. Billings and I. M. Ritchie, *Electrochim. Acta* **25** (1980) 733.